Ambident Reactivities of Pyridone Anions

Martin Breugst and Herbert Mayr*

Department Chemie, Ludwig-Maximilians-Universität, Butenandtstrasse 5-13, 81377 München, Germany

Received August 4, 2010; E-mail: Herbert.Mayr@cup.uni-muenchen.de

Abstract: The kinetics of the reactions of the ambident 2- and 4-pyridone anions with benzhydrylium ions (diarylcarbenium ions) and structurally related Michael acceptors have been studied in DMSO, CH_3CN, and water. No significant changes of the rate constants were found when the counterion was varied (Li^+, K^+, NBu_4^+) or the solvent was changed from DMSO to CH_3CN, whereas a large decrease of nucleophilicity was observed in aqueous solution. The second-order rate constants ($\log k_2$) correlated linearly with the electrophilicity parameters E of the electrophiles according to the correlation $\log k_2 = s(N + E)$ (*Angew. Chem., Int. Ed. Engl.* **1994**, *33*, 938−957), allowing us to determine the nucleophilicity parameters N and s for the pyridone anions. The reactions of the 2- and 4-pyridone anions with stabilized amino-substituted benzhydrylium ions and Michael acceptors are reversible and yield the thermodynamically more stable *N*-substituted pyridones exclusively. In contrast, highly reactive benzhydrylium ions (4,4′-dimethylbenzhydrylium ion), which react with diffusion control, give mixtures arising from *N*- and *O*-attack with the 2-pyridone anion and only *O*-substituted products with the 4-pyridone anion. For some reactions, rate and equilibrium constants were determined in DMSO, which showed that the 2-pyridone anion is a 2−4 times stronger nucleophile, but a 100 times stronger Lewis base than the 4-pyridone anion. Quantum chemical calculations at MP2/6-311+G(2d,p) level of theory showed that *N*-attack is thermodynamically favored over *O*-attack, but the attack at oxygen is intrinsically favored. Marcus theory was employed to develop a consistent scheme which rationalizes the manifold of regioselectivities previously reported for the reactions of these anions with electrophiles. In particular, Kornblum's rationalization of the silver ion effect, one of the main pillars of the hard and soft acid/base concept of ambient reactivity, has been revised. Ag^+ does not reverse the regioselectivity of the attack at the 2-pyridone anion by increasing the positive charge of the electrophile but by blocking the nitrogen atom of the 2-pyridone anion.

Introduction

The anions of 2-pyridone (**1**) and 4-pyridone (**2**) are possibly the least understood ambident nucleophiles. As the selective formation of *N*-alkylated pyridones and alkoxypyridines according to Scheme 1 is of eminent importance for the synthesis of many biologically active compounds,[1] control of the regioselectivitiy of electrophilic attack at **1** and **2** has intrigued chemists for many decades.[2]

Kornblum rationalized the predominant formation of 2-ethoxypyridine from the silver salt of 2-pyridone with ethyl iodide by the "great carbonium character" of the electrophile in the presence of silver ions.[3] Systematic investigations of the alkylations of 2-pyridone salts by Tieckelmann[4] showed "*that the results are completely consistent with Kornblum's proposal*

Scheme 1. Ambident Reactivities of Pyridone Anions
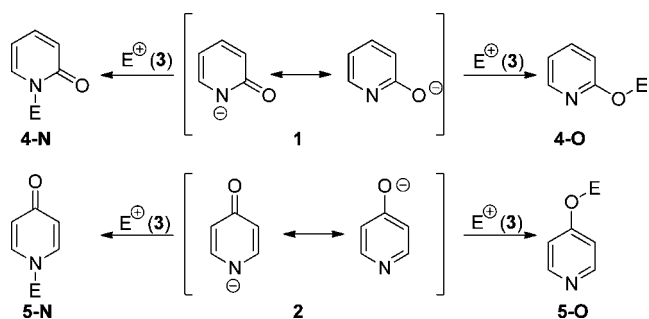
that the silver ion enhances unimolecular character in the silver salt reactions, thereby favoring alkylation at the more electronegative oxygen atom".[4a] However, at the end of his thorough investigation, Tieckelmann stated: "*The mechanism which leads to oxygen alkylation of the silver salts of 2-pyridones also needs further examination and may be more related to heterogeneous reaction than to the ability of the silver ion to promote unimolecular reaction as previously suggested*".[4a]

Kornblum's rule was later integrated in Pearson's concept of "Hard and Soft Acids and Bases" (HSAB) which became

(1) (a) Comins, D. L.; Baevsky, M. F.; Hong, H. *J. Am. Chem. Soc.* **1992**, *114*, 10971–10972. (b) Liu, H.; Ko, S.-B.; Josien, H.; Curran, D. P. *Tetrahedron Lett.* **1995**, *36*, 8917–8920. (c) Conreaux, D.; Bossharth, E.; Monteiro, N.; Desbordes, P.; Balme, G. *Tetrahedron Lett.* **2005**, *46*, 7917–7920. (d) Tipparaju, S. K.; Joyasawal, S.; Forrester, S.; Mulhearn, D. C.; Pegan, S.; Johnson, M. E.; Mesecar, A. D.; Kozikowski, A. P. *Bioorg. Med. Chem. Lett.* **2008**, *18*, 3565–3569.

(2) (a) Meislich, H. In *Pyridine and Its Derivatives, Part III*; Klingsberg, E., Ed.; Interscience Publisher: New York, 1962; pp 511−890. (b) Keller, P. A. In *Science of Synthesis, Vol. 15*; Thieme: Stuttgart, **2005**; pp 285−387.

(3) Kornblum, N.; Smiley, R. A.; Blackwood, R. K.; Iffland, D. C. *J. Am. Chem. Soc.* **1955**, *77*, 6269–6280.

(4) (a) Hopkins, G. C.; Jonak, J. P.; Minnemeyer, H. J.; Tieckelmann, H. *J. Org. Chem.* **1967**, *32*, 4040–4044. (b) Chung, N. M.; Tieckelmann, H. *J. Org. Chem.* **1970**, *35*, 2517–2520.

Table 1. Reference Electrophiles Employed in this Work and Wavelengths Monitored in the Kinetic Experiments

Electrophile			E^a	λ/nm
	R = H	**3a**	+5.90	—
	R = Me	**3b**	+3.63	—
	R = NMe$_2$	**3c**	−7.02	613
	R = N(CH$_2$)$_4$	**3d**	−7.69	620
	n = 2	**3e**	−8.22	618
	n = 1	**3f**	−8.76	627
	n = 2	**3g**	−9.45	635
	n = 1	**3h**	−10.04	630
	R = OMe	**3i**	−12.18	422
	R = NMe$_2$	**3j**	−13.39	533
	R = 4-NO$_2$	**3k**	−14.32	374
	R = 4-Me	**3l**	−15.83	371
	R = 4-OMe	**3m**	−16.11	393
	R = 4-NMe$_2$	**3n**	−17.29	486
		3o	−17.90	521

^{a} Electrophilicity parameters from ref 7.

the best known approach to rationalize ambient reactivity in general.[5] Remarkably few investigators have employed the HSAB model on the pyridone anions,[6] and a consistent rationalization of the large diversity of experimental results with **1** and **2** is lacking despite the great importance of these anions in synthesis.

Systematic experimental investigations of the reactivities of cyanide,[8] cyanate,[9] thiocyanate,[10] nitrite,[11] and phenyl sulfinate[12] demonstrated that not even the behavior of the prototypes of ambient nucleophiles can be explained by the HSAB model[5] or the related Klopman–Salem concept of charge and orbital controlled reactions.[13] Recently, we have shown that Marcus theory[14] provides a consistent rationalization of the ambient
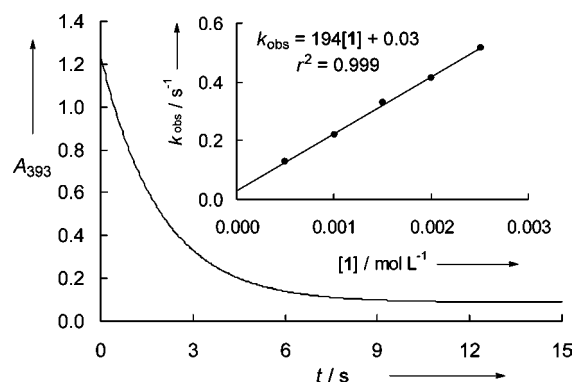
Figure 1. Plot of the absorbance at 393 nm, A_{393}, vs time for the reaction of **3m** with the anion of 2-pyridone (**1**) in DMSO at 20 °C and correlation of the first-order rate constants k_{obs} with the concentration of **1** (inset).

reactivities of these nucleophiles.[15] We now report on a systematic experimental and quantum chemical investigation of the ambient reactivities of **1** and **2**, and demonstrate that Marcus theory also provides a consistent rationalization of the ambient reactivities of pyridone anions.

In previous work, we have shown that the benzhydrylium ions **3a–h** and the structurally related quinone methides **3i–o** (Table 1) are electrophiles, which differ by approximately 20 orders of magnitude in reactivity while the steric surroundings of the reaction center are kept constant.[7] We now use these compounds as reference electrophiles to investigate the influence of electrophilicity on regioselectivity and kinetics of the reactions of the pyridone anions **1** and **2**.

Results

Kinetic Investigations. The reactions of the pyridone anions **1** and **2** with the quinone methides **3i–o** and the benzhydrylium ions **3d–h** were performed in DMSO, acetonitrile, or water at 20 °C and monitored by UV–vis spectroscopy at or close to the absorption maxima of the electrophiles (354 < λ < 635 nm) (Table 1). While the anions of 2-pyridone (**1**) reacted smoothly with the quinone methides **3k–o**, no reactions were observed when the anion of 4-pyridone (**2**) was employed. Reactivities of the more electrophilic benzhydrylium ions **3a–c** could not be determined, because the laser-flash-photolytic generation of benzhydrylium ions, which we usually employ for studying fast reactions, was not applicable due to the absorption of the pyridone anions **1** and **2** ($\varepsilon = 1.85 \times 10^3$ L mol^{-1} cm^{-1}) at 266 nm, i.e., the excitation wavelength of the laser.

By using the nucleophiles **1** and **2** in large excess over the electrophiles, their concentrations remained almost constant throughout the reactions, and pseudo-first-order kinetics were obtained in all runs. The first-order rate constants k_{obs} were then

(5) (a) Pearson, R. G. *J. Am. Chem. Soc.* **1963**, *85*, 3533–3539. (b) Pearson, R. G. *Science* **1966**, *151*, 172–177. (c) Pearson, R. G. *J. Chem. Educ.* **1968**, *45*, 581–587. (d) Pearson, R. G. *J. Chem. Educ.* **1968**, *45*, 643–648. (e) Pearson, R. G. *Chemical Hardness*; Wiley-VCH: Weinheim, 1997.

(6) (a) Zaragoza Dörwald, F. *Side Reactions in Organic Synthesis*; Wiley-VCH: Weinheim, 2005, pp 1–16. (b) Ho, T.-L. *Chem. Rev.* **1975**, *75*, 1–20.

(7) (a) Mayr, H.; Bug, T.; Gotta, M. F.; Hering, N.; Irrgang, B.; Janker, B.; Kempf, B.; Loos, R.; Ofial, A. R.; Remennikov, G.; Schimmel, H. *J. Am. Chem. Soc.* **2001**, *123*, 9500–9512. (b) Lucius, R.; Loos, R.; Mayr, H. *Angew. Chem., Int. Ed.* **2002**, *41*, 91–95. (c) Richter, D.; Hampel, N.; Singer, T.; Ofial, A. R.; Mayr, H. *Eur. J. Org. Chem.* **2009**, 3203–3211.

(8) Tishkov, A. A.; Mayr, H. *Angew. Chem., Int. Ed.* **2005**, *44*, 142–145.

(9) Schaller, H. F.; Schmidhammer, U.; Riedle, E.; Mayr, H. *Chem.—Eur. J.* **2008**, *14*, 3866–3868.

(10) Loos, R.; Kobayashi, S.; Mayr, H. *J. Am. Chem. Soc.* **2003**, *125*, 14126–14132.

(11) Tishkov, A. A.; Schmidhammer, U.; Roth, S.; Riedle, E.; Mayr, H. *Angew. Chem., Int. Ed.* **2005**, *44*, 4623–4626.

(12) Baidya, M.; Kobayashi, S.; Mayr, H. *J. Am. Chem. Soc.* **2010**, *132*, 4796–4805.

(13) (a) Klopman, G. *J. Am. Chem. Soc.* **1968**, *90*, 223–234. (b) Salem, L. *J. Am. Chem. Soc.* **1968**, *90*, 543–552.

(14) (a) Marcus, R. A. *Annu. Rev. Phys. Chem.* **1964**, *15*, 155–196. (b) Marcus, R. A. *Pure Appl. Chem.* **1997**, *69*, 13–29.

(15) Breugst, M.; Zipse, H.; Guthrie, J. P.; Mayr, H. *Angew. Chem., Int. Ed.* **2010**, *49*, 5165–5169.

derived by least-squares fitting of the time-dependent absorbances A_t of the electrophiles to the exponential function $A_t = A_0\exp(-k_{obs}t) + C$. Second-order rate constants were obtained as the slopes of the plots of k_{obs} versus the concentration of the nucleophiles (Figure 1).

Due to the low acidities of the pyridones **1-H** ($pK_a = 11.74$)[16a] and **2-H** ($pK_a = 11.12$),[16a] aqueous solutions of the pyridone anions **1** and **2** are partially hydrolyzed and contain hydroxide anions. For that reason, three competing reactions may account for the decay of the benzhydrylium ions in water and the observed rate constants k_{obs} for the consumption of the electrophiles in water reflect the sum of their reactions with the pyridone anions **1** or **2** (k_2), hydroxide ($k_{2,OH}$),[17] and water (k_w) (eq 1).

$$k_{obs} = k_2[\mathbf{1} \text{ or } \mathbf{2}] + k_{2,OH}[OH^-] + k_w \qquad (1)$$

$$k_{eff} = k_{obs} - k_{2,OH}[OH^-] = k_2[\mathbf{1} \text{ or } \mathbf{2}] + k_w \qquad (2)$$

All equilibrium concentrations in eq 2 were calculated from the initial concentrations and the pK_{aH} values, as described in the Supporting Information. Rearrangement of eq 1, i.e., subtraction of the contribution of hydroxide from the observed rate constant k_{obs}, yields eq 2, and the second-order rate constants for the reactions of the benzhydrylium ions with **1** and **2** can then be obtained from plots of k_{eff} versus the concentration of the nucleophiles. By combining the pyridones **1-H** and **2-H**, which are used in high excess over the electrophiles **3** (pseudo-first-order conditions), with only 0.02−0.2 equiv of KOH, we were able to realize conditions, where the correction term $k_{2,OH}[OH^-]$ never exceeded 10% of k_{obs}, thus giving rise to highly reliable values of k_2. The intercepts of these plots correspond to the reactions of the electrophiles with water and are generally negligible in agreement with previous work, where water ($N = 5.20$)[18] was demonstrated to react much more slowly with benzhydrylium ions than the nucleophiles investigated in this work.

As shown for several examples in the Supporting Information, k_{obs} values obtained for **1-K** and **2-K** in the presence and in the absence of 18-crown-6 are on the same k_{obs} vs [**1**] or k_{obs} vs [**2**] plots, indicating that in the concentration range under investigation ($c < 4 \times 10^{-3}$ M) reactivities of the free anions **1** (Table 2) and **2** (Table 3) are observed.

Furthermore, an exchange of K$^+$ by Li$^+$ only moderately reduces the rate constant in DMSO by a factor of 0.65 (Table 2), in line with previous findings by Tieckelmann.[4]

Solvent Effects. Tables 2 and 3 show that the reactivities of **1** and **2** toward benzhydrylium ions and quinone methides (**3**) are almost identical in DMSO and CH$_3$CN. The rate constants in these solvents differ by less than a factor of 1.5, and we can neglect differential solvent effects when comparing rate constants determined in DMSO and CH$_3$CN. The rate constants for the reaction of **1** and **2** with benzhydrylium ions show a different order in DMSO and water. As depicted in Scheme 2 for the reactions with **3h**, 2-pyridone anion (**1**) reacts approximately 48000 times faster in DMSO than in water, while the reactions of 4-pyridone anion (**2**) differ by a factor of only ~2000. The resulting reversal of the relative reactivities of **1**

(16) (a) pK_a in H$_2$O Bunting, J. W.; Toth, A.; Heo, C. K. M.; Moors, R. G. *J. Am. Chem. Soc.* **1990**, *112*, 8878–8885. (b) pK_a in DMSO: **1-H**: 17.0, **2-H**: 14.8 Bordwell, F. G. *Acc. Chem. Res.* **1988**, *21*, 456–463.
(17) Minegishi, S.; Mayr, H. *J. Am. Chem. Soc.* **2003**, *125*, 286–295.

Table 2. Second-Order Rate Constants for the Reactions of the 2-Pyridone Anion **1** with Reference Electrophiles at 20 °C

| solvent	N/s	electrophile	k_2/L mol^{-1} s^{-1}
DMSO	19.91/0.60	**3o**	1.51×10^1
		3n	3.68×10^1
		3m	1.94×10^2
		3l	2.44×10^2
			$1.66 \times 10^{2,a}$
		3k	3.06×10^3
		3j	6.49×10^3
		3i	4.05×10^4
			$2.64 \times 10^{4,a}$
		3h	8.69×10^5
		3g	1.65×10^6
CH$_3$CN	20.11/0.57	**3o**	1.94×10^1
		3n	3.84×10^1
		3m	1.72×10^2
		3l	2.38×10^2
		3k	2.34×10^3
		3j	5.79×10^3
		3i	3.12×10^4
water	12.47/0.52	**3h**	2.04×10^1
		3g	3.42×10^1
		3f	8.50×10^1
		3e	1.56×10^2
		3d	3.37×10^2

^{a} Li$^+$ as counterion.

Table 3. Second-Order Rate Constants for the Reactions of the 4-Pyridone Anion **2** with Reference Electrophiles at 20 °C

| solvent	N/s	electrophile	k_2/L mol^{-1} s^{-1}
DMSO	18.97/0.62	**3k**	7.28×10^2
		3j	2.75×10^3
		3i	1.34×10^4
		3h	3.26×10^5
		3g	7.45×10^5
CH$_3$CN	20.22/0.49	**3l**	1.61×10^2
		3k	5.53×10^2
		3j	2.25×10^3
		3i	9.14×10^3
water	14.76/0.48	**3h**	1.93×10^2
		3g	2.99×10^2
		3f	6.61×10^2
		3e	1.35×10^3
		3d	2.34×10^3

Scheme 2. Solvent Dependence of the Rate Constant of the Reactions of **1-K** and **2-K** with **3h** at 20 °C and the Corresponding pK_a Values (pK_a from ref 16)
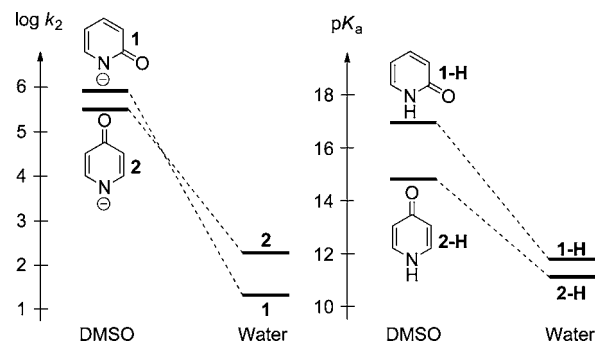
and **2** in the two solvents indicates that the 2-pyridone anion **1** is better stabilized by hydrogen bonding in water than the 4-pyridone anion **2**. In line with this interpretation the significant

(18) Minegishi, S.; Kobayashi, S.; Mayr, H. *J. Am. Chem. Soc.* **2004**, *126*, 5174–5181.
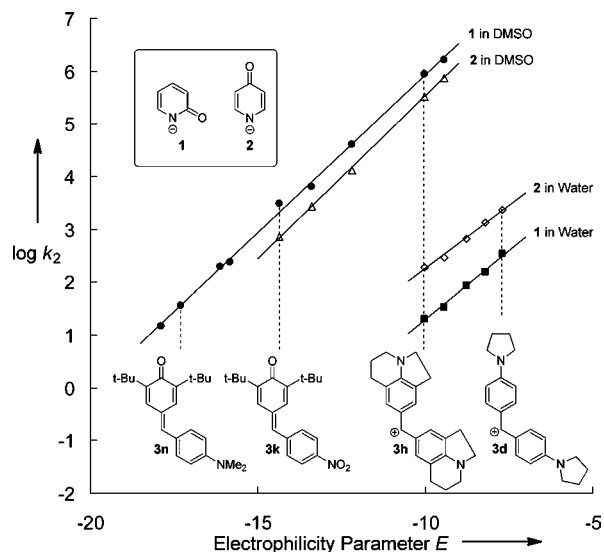
Figure 2. Plots of the rate constants log k_2 for the reaction of the pyridone anions **1** and **2** with reference electrophiles versus their electrophilicity parameters E (correlation in CH₃CN are shown in the Supporting Information).

difference between the acidities of 2-pyridone (**1-H**) and 4-pyridone (**2-H**) in DMSO is almost canceled in aqueous solution (Scheme 2, right).

Correlation Analysis. In line with the linear free-energy relationship (eq 3), where the second-order rate constant (log k_2) is described by the nucleophile-specific parameters s and N and the electrophile-specific parameter E,[19] plots of log k_2 for the reactions of the pyridone anions **1** and **2** with the reference electrophiles **3d−o** versus their electrophilicity parameters E were linear.

$$\log k_2 = s(N + E) \quad (3)$$

The slopes of these correlations correspond to the nucleophile-specific sensitivity parameters s, whereas the negative intercepts on the abscissa yield the nucleophilicity parameters N. For reasons of clarity the rate constants determined in CH₃CN are not shown in Figure 2, but all individual correlations are depicted in the Supporting Information. The almost parallel correlation lines in Figure 2 which refer to N-attack (see below) imply that the relative reactivities of 2- and 4-pyridone anions (**1** and **2**) are nearly independent of the reactivities of the electrophiles.

Reaction Products. Scheme 3 specifies the general Scheme 1 for the reaction of the pyridone anions **1** and **2** with the benzhydrylium ions **3a−h** and the quinone methides **3i−o**. The letters in the products **4** and **5** identify their origin; thus, **4k-N** is formed from **1** and **3k** via N-attack.

When the potassium salts of **1** or **2** (1 to 5 equiv) were combined with the quinone methides **3l** and **3k** in dry DMSO or dry CH₃CN, the solutions remained colored, indicating incomplete reactions. Equilibria and nonoptimized workup procedures account for the fact that some reaction products were only obtained in moderate yields (Table 5). The reactions of **1** and **2** with the weakly stabilized benzhydrylium ions **3c−h** resulted in colorless solutions, but as the investigated pyridone anions **1** and **2** are weak bases in water (pK_{aH}(**1**) = 11.74 and pK_{aH}(**2**) = 11.12),[16a] the resulting products undergo heterolytic cleavage during aqueous workup. In these cases, product studies

(19) Mayr, H.; Patz, M. *Angew. Chem., Int. Ed. Engl.* **1994**, *33*, 938–957.

**Scheme 3.** Reaction of Pyridone Anions **1** and **2** with the Electrophiles **3a−o** in DMSO
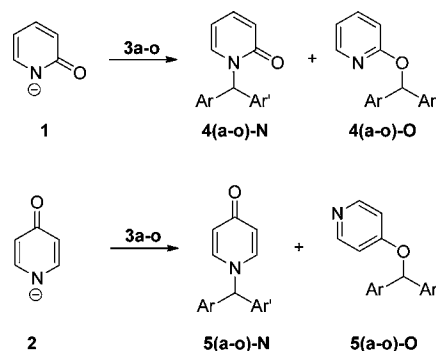
were performed by NMR spectroscopy in d^6-DMSO solution (see the Supporting Information for NMR spectra).

The carbonyl carbon of the 4-pyridones (δ 177.4 for **5g-N**) is considerably more deshielded than the oxy-substituted 4-position of the 4-oxysubstituted pyridines (δ 164 for **5a-O** and **5b-O**) which allows a straightforward differentiation of the two isomers.

In contrast, the carbonyl group of the 2-pyridones **4(a−o)-N** and the alkoxy-substituted ring carbon in the pyridines **4(a−o)-O** have similar ^{13}C NMR chemical shifts. Therefore, the site of attack at the 2-pyridone anion **1** cannot directly be derived from the appearance of a ^{13}C NMR signal for the carbonyl group, and the differentiation between N- and O-alkylated products was based on 2D-NMR experiments.

In cases where the reaction products are isolable, the structural assignment can be confirmed by IR-spectroscopy. While the N-alkylated pyridones **4l-N**, **4k-N**, **4b-N**, and **4a-N** show a strong band at ∼1660 cm⁻¹, the alkoxypyridines **4a-O** and **5a-O** absorb at ∼1590 cm⁻¹. Further structural evidence comes from the crystal structure of **4l-N** (Figure 3, Table 4).

Independent of the counterion and the solvent, the anion of 2-pyridone (**1**) gives exclusive N-alkylation with the quinone methides **3l** and **3k** and with the weakly electrophilic benzhydrylium ions **3c** and **3g** (Table 5, entries 1−7). Mixtures resulting from O- and N-attack were obtained, when **1** was treated with the tetrafluoroborate of the more electrophilic ditolylcarbenium ion **3b** (entry 8) or the corresponding benz-
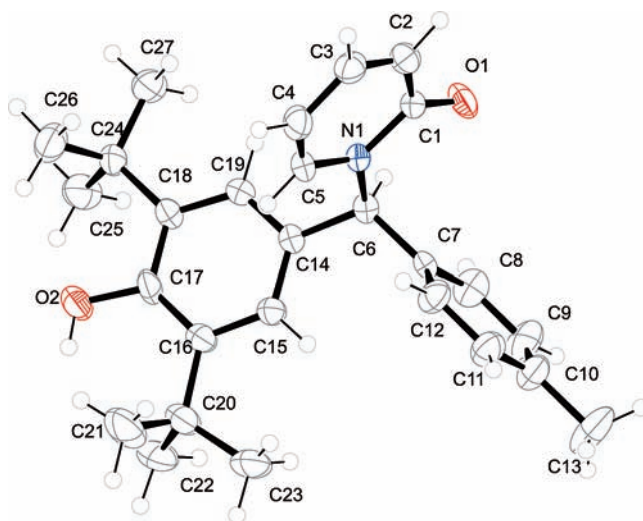
Figure 3. Crystal structure of the reaction product **4l-N** obtained from **1a-K** and **2l** (50% probability ellipsoids).

Table 4. Crystallographic Data of **4l-N**

empirical formula	$C_{27}H_{33}NO_2$
M_r/g mol^{-1}	403.556
crystal size/mm	$0.41 \times 0.10 \times 0.09$
T/K	173(2)
radiation	MoKα
diffractometer	Oxford XCalibur
crystal system	monoclinic
space group	$P2_1/c$
a/Å	10.6093(6)
b/Å	10.9456(8)
c/Å	20.9242(13)
α/deg	90
β/deg	94.074(5)
γ/deg	90
V/Å^3	2423.7(3)
Z	4
calc. density/g cm^{-3}	1.10596(14)
μ/mm^{-1}	0.069
absorption correction	'multiscan'
transmission factor range	0.95407−1.00000
reflections measured	9587
R_{int}	0.0884
mean $\sigma(I)/I$	0.1934
θ range	4.19−25.37
observed reflections	1693
x, y (weighting scheme)	0.0293, 0
hydrogen refinement	constr
reflections in refinement	4391
parameters	278
restraints	0
$R(F_{obs})$	0.0563
$R_w(F^2)$	0.1005
S	0.776
shift/error$_{max}$	0.001
max electron density/e Å^{-3}	0.153
min electron density/e Å^{-3}	−0.147

Scheme 4. Products of the Reactions of the Pyridone Anions **1** and **2** with the Michael Acceptors **6** and **7**

6a,b

7a−c

Reactions with Other Types of Michael Acceptors. NMR studies showed that the Michael acceptors **6a,b** and **7a−c** also exclusively attack the nitrogen atom of the pyridone anions **1** and **2** and that oxygen attack did not occur (Scheme 4). Comparison of the experimentally determined rate constants (Table 6) with those calculated by eq 3 from the *N*/*s*-parameters of **1** and **2** (Tables 2 and 3) and the previously published electrophilicity parameters[20] of **6a,b** and **7a−c** is an impressive demonstration of the predictive power of the three-parameter eq 3, which presently covers 40 orders of magnitude. While the calculated rate constants for **1** are 1.5−3 times larger than the experimental values, k_{calc} for **2** are 2.5−7 times smaller than the experimental numbers.

Equilibrium Constants and Intrinsic Barriers. In DMSO the pyridone anions **1** and **2** reacted quantitatively with all investigated benzhydrylium ions and with quinone methides of $E > -14$, while incomplete reactions were observed with less reactive electrophiles. As the quinone methides are colored and the reaction products are colorless, we were able to determine equilibrium constants for these reactions (Table 7) by UV/vis spectrometry as described on pp S4 and S41−46 of the Supporting Information.
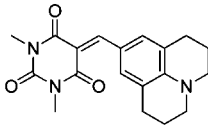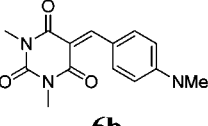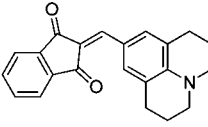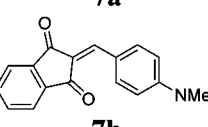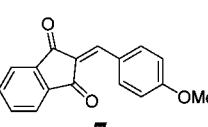
The availability of rate and equilibrium constants allows us to employ Marcus theory[14] (eq 4) for calculating the intrinsic

hydryl bromides **3b-Br** and **3a-Br** (entries 9−10, 12). Only when the silver salt of **1** was treated with **3b-Br**, exclusive *O*-attack took place (entry 11).

A different behavior was found for the 4-pyridone anion (**2**). While the weakly electrophilic benzhydrylium ion **3g** gave exclusive *N*-attack (entry 14), only alkoxypyridines were isolated in the reactions of **2** with the more electrophilic benzhydrylium ion **3b** or the corresponding benzhydrylium bromides **3b-Br** and **3a-Br** (entries 15−18).

Table 5. Products of the Reactions of the Pyridone Salts (**1** and **2**) with Electrophiles

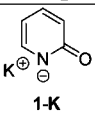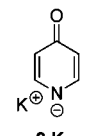|		electrophile			product (yield %)	
entry	pyridone	No	E^a	solvent	*N*-attack	*O*-attack
1	**1-K**	**3l**	−15.83	DMSO	**4l-N** (88%)	−
2	**1-Li**	**3l**	−15.83	DMSO	**4l-N** (80%)	−
3	**1-K**	**3l**	−15.83	CH$_3$CN	**4l-N** (79%)	−
4	**1-NBu$_4$**	**3l**	−15.83	CH$_3$CN	**4l-N** (89%)	−
5	**1-K**	**3k**	−14.32	DMSO	**4k-N** (84%)	−
6	**1-K**	**3g**	−9.45	DMSO	**4g-N** (NMR)	−
7	**1-K**	**3c**	−7.02	DMSO	**4c-N** (NMR)	−
8	**1-K**	**3b**^{b}	+3.63	CH$_3$CN/CH$_2$Cl$_2$	**4b-N** (49%)^c	**4b-O** (17%)
9	**1-NBu$_4$**	**3b-Br**	+3.63	CH$_3$CN	**4b-N** (50%)	**4b-O** (38%)
10	**1-NBu$_4$**	**3b-Br**	+3.63	CH$_3$CN/H$_2$O (9:1)	**4b-N**(53%)	**4b-O** (41%)
11	**1-Ag**^{d}	**3b-Br**	+3.63	CH$_3$CN	−	**4b-O** (92%)
12	**1-NBu$_4$**	**3a-Br**	+5.90	CH$_3$CN	**4a-N** (60%)	**4a-O** (38%)
13	**2-K**	**3l**	−15.83	DMSO	no reaction	
14	**2-K**	**3g**	−9.45	DMSO	**5g-N** (NMR)	−
15	**2-K**	**3b**	+3.63	CH$_3$CN/CH$_2$Cl$_2$	−	**5b-O** (74%)
16	**2-NBu$_4$**	**3b-Br**	+3.63	CH$_3$CN	−	**5b-O** (71%)
17	**2-Ag**^{d}	**3b-Br**	+3.63	CH$_3$CN	−	**5b-O** (72%)
18	**2-NBu$_4$**	**3a-Br**	+5.90	CH$_3$CN	−	**5a-O** (77%)

^{a} Empirical electrophilicity parameters from ref 7. ^{b} **3b-Br** was ionized with 1 equiv of AgOTf; as AgBr precipitates, there are no Ag$^+$ ions in solution. ^{c} Along with 31% (tol$_2$CH)$_2$O. ^{d} **3b-Br** was added to heterogeneous systems obtained by treatment of **1-NBu$_4$** or **2-NBu$_4$** with AgNO$_3$.

Table 6. Rate Constants (in L mol^{-1} s^{-1}) for the Reactions of **1** and **2** with Michael Acceptors **6** and **7** at 20 °C

Electrophile	E^a	Pyridone	Solvent	$k_{2,\text{exp}}$	$k_{2,\text{calc}}$
6a	−13.97	1	DMSO	1.27×10^3	3.7×10^3
			CH$_3$CN	1.35×10^3	3.2×10^3
		2	DMSO	6.51×10^3	1.3×10^3
			CH$_3$CN	7.58×10^3	1.2×10^3
6b	−12.76	1	DMSO	7.54×10^3	1.9×10^4
			CH$_3$CN	8.98×10^3	1.5×10^4
		2	DMSO	3.02×10^4	7.1×10^3
			CH$_3$CN	3.10×10^4	4.5×10^3
7a	−14.68	1	DMSO	8.03×10^2	1.4×10^3
			CH$_3$CN	5.79×10^2	1.2×10^3
		2	DMSO	2.45×10^3	4.6×10^2
			CH$_3$CN	1.51×10^3	5.2×10^2
7b	−13.56	1	DMSO	3.59×10^3	6.5×10^3
			CH$_3$CN	2.73×10^3	5.4×10^3
		2	DMSO	8.02×10^3	2.3×10^3
			CH$_3$CN	6.64×10^3	1.8×10^3
7c	−11.32	1	DMSO	7.60×10^4	1.4×10^5
			CH$_3$CN	6.50×10^4	1.0×10^5
		2	DMSO	1.37×10^5	5.5×10^4
			CH$_3$CN	7.98×10^4	2.3×10^4

^{a} Electrophilicities E from ref 20.

Table 7. Equilibrium Constants, Gibbs Reaction Energies ΔG^0, Gibbs Activation Energies $\Delta G^\ddagger$, and Intrinsic Barriers $\Delta G_0^\ddagger$ for the Reactions of Pyridone Anions with Electrophiles in DMSO at 20 °C (all energies in kJ mol^{-1})

Nucleophile	Electrophile	K / L mol^{-1}	ΔG^0	$\Delta G^{\ddagger,a}$	$\Delta G_0^{\ddagger,b}$
1-K	3l	$(1.40 \pm 0.09) \times 10^4$	−23.3	58.4	69.6
	3m	$(6.15 \pm 0.24) \times 10^3$	−21.3	58.9	69.1
	3n	$(3.56 \pm 0.30) \times 10^2$	−14.3	63.0	70.0
	3o	$(9.91 \pm 0.66) \times 10^1$	−11.2	65.1	70.6
2-K	3k	$(1.27 \pm 0.06) \times 10^3$	−17.4	55.7	64.1
	3l	$(8.18 \pm 0.49) \times 10^1$	−10.7	$\sim 61^c$	~ 66
	3m	$(4.27 \pm 0.23) \times 10^1$	−9.2	$\sim 62^c$	~ 66
	7a	$(1.82 \pm 0.05) \times 10^3$	−18.3	52.7	61.5

^{a} From Tables 2, 3, and 6 using the Eyring equation (eq 5). ^{b} From eq 4. ^{c} $\Delta G^\ddagger$ was calculated from k_2 obtained from eq 3 with N/s from Table 3 and $E(\mathbf{3})$ from Table 1.

barriers $\Delta G_0^\ddagger$ (defined as the activation energy for a thermoneutral reaction, Table 7) from the Gibbs energy of activation $\Delta G^\ddagger$ (derived from the rate constants, eq 5) and the Gibbs energy of reaction ΔG^0 (derived from the equilibrium constants, eq 6).

$$\Delta G^\ddagger = \Delta G_0^\ddagger + 0.5\Delta G^0 + \left[(\Delta G^0)^2/16\Delta G_0^\ddagger\right] \quad (4)$$

$$\Delta G^\ddagger = -RT \ln[(kh)/(k_\text{b}T)] \quad (5)$$

$$\Delta G^0 = -RT \ln K \quad (6)$$

Table 7 shows that the equilibrium constants for the reactions of **1** with quinone methides in DMSO are more than 2 orders of magnitude larger than those of analogous reactions of **2**. On the other hand, **1** reacts only 2−4 times faster than **2** with neutral (**3i**−**k**) and charged electrophiles (**3g,h**) in DMSO. Obviously, the reactions of the 2-pyridone anion **1** require a considerably higher reorganization energy than the analogous reactions of the 4-pyridone anion **2**, as quantitatively expressed by the intrinsic barriers $\Delta G_0^\ddagger$ in the last column of Table 7.

Quantum Chemical Calculations. Extending earlier work by Wolfe and Schlegel,[21] as well as by Schaefer,[22] we have recently demonstrated that the directly calculated activation energies of C- and O-alkylation of enolate anions with methyl halides agree well with those derived from eq 4 using calculated Gibbs

reaction energies ΔG^0 and intrinsic barriers $\Delta G_0^{\ddagger}$ which were obtained as the arithmetic mean of the corresponding identity reactions.[15] Calculated values of ΔG^0 and $\Delta G_0^{\ddagger}$ for the methylation of enolate, cyanide, cyanate, thiocyanate, and nitrite in combination with the Marcus equation were reported to provide a consistent rationalization of the ambident reactivities of these nucleophiles.

In order to employ this method also on the ambident reactivities of the pyridone anions **1** and **2**, we have calculated the Gibbs energies of activation for the identity methyl-transfer reactions in eqs 7−10 at the MP2/6-311+G(2d,p) level, as this method was found to give similar results as G3(+) calculations of related systems.[15] The barriers for *O*-attack (97.5 and 85.9 kJ mol^{-1}, eqs 8, 10) are smaller than the corresponding barriers for the attack at nitrogen (108 and 93.4 kJ mol^{-1}, eqs 7, 9) which is in agreement with Hoz's findings that the barriers of identity S_N2 reactions decrease when the center of nucleophilicity is positioned further right in the periodic table.[23] Intrinsically preferred is, hence, oxygen attack in the reactions of 2- and 4-pyridone anions.

Comparison of eqs 7 and 9 as well of eqs 8 and 10 furthermore shows that the reactions of the 4-pyridone anion **2** are intrinsically favored over the corresponding reactions of the 2-pyridone anion **1**, a trend which is also observed experimentally in reactions with the electrophiles **3** (see Table 7).
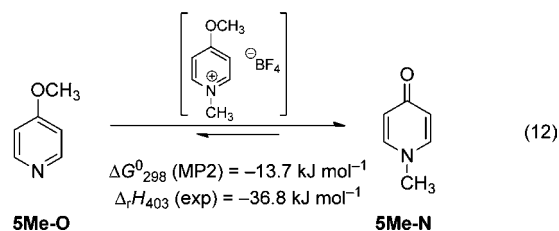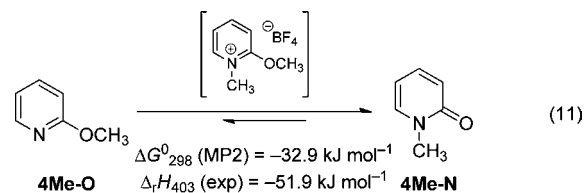
(7)

(8)

(9)

(10)
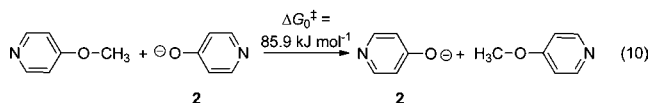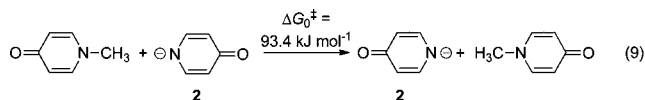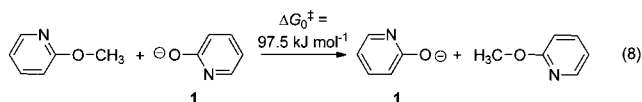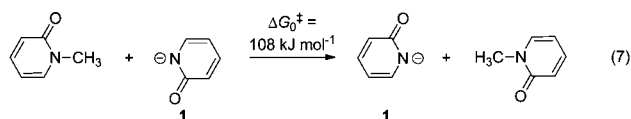
Furthermore, we have calculated the Gibbs reaction energies for the methylation of the ambident pyridone anions **1** and **2** with methyl chloride at MP2/6-311+G(2d,p) level of theory. Table 8 shows that the *N*-methyl pyridones are thermodynamically favored over the corresponding methoxypyridines by 32.9 kJ mol^{-1} (for 2-pyridone) and 13.7 kJ mol^{-1} (for 4-pyridone). In agreement with these calculations, calorimetric measurements by Beak showed that the rearrangement **4Me-O → 4Me-N** (eq 11) is considerably more exothermic than the analogous rearrangement in the 4-pyridone series (eq 12).[24] The absolute values of the experimental enthalpies of rearrangement are considerably larger than the calculated numbers as specified in eqs 11 and 12, but the differences of the two series ($\Delta\Delta_r H$) are similar (19.2 kJ mol^{-1} calculated gas phase vs 15.1 kJ mol^{-1} calorimetric).

Table 8. Intrinsic Barriers, Reaction Free Energies, and Activation Free Energies for the Methylation of Pyridone Anions **1** and **2** by Methyl Chloride in the Gas Phase (MP2/6-311+G(2d,p), in kJ mol^{-1})

	$\Delta G_0^{\ddagger a}$	ΔG^0	$\Delta G^{\ddagger}$
	+72.9	−66.7	+43.4
	+67.9	−33.8	+52.1
	+65.8	−12.8	+59.6
	+62.0	+0.9	+62.4

^{a} $\Delta G_0^{\ddagger} = 0.5[\Delta G_0^{\ddagger}$ (eqs 7−10) $+\Delta G_0^{\ddagger}$ (Cl$^-$ + MeCl)].

ΔG^0_{298} (MP2) = −32.9 kJ mol^{-1}
$\Delta_r H_{403}$ (exp) = −51.9 kJ mol^{-1}

(11)

ΔG^0_{298} (MP2) = −13.7 kJ mol^{-1}
$\Delta_r H_{403}$ (exp) = −36.8 kJ mol^{-1}

(12)

Using Marcus' additivity rule,[25] which yields the intrinsic barriers for nonidentity reactions as the arithmetic means of the corresponding identity reactions, $\Delta G_0^{\ddagger}$ for the reactions of **1** and **2** with CH$_3$Cl (Table 8) are obtained from the identity reactions in eqs 7−10 and the intrinsic barrier for the chloride

(20) (a) Seeliger, F.; Berger, S. T. A.; Remennikov, G. Y.; Polborn, K.; Mayr, H. *J. Org. Chem.* **2007**, *72*, 9170–9180. (b) Berger, S. T. A.; Seeliger, F.; Hofbauer, F.; Mayr, H. *Org. Biomol. Chem.* **2007**, *5*, 3020–3026.

(21) (a) Wolfe, S.; Mitchell, D. J.; Schlegel, H. B. *J. Am. Chem. Soc.* **1981**, *103*, 7692–7694. (b) Wolfe, S.; Mitchell, D. J.; Schlegel, H. B. *J. Am. Chem. Soc.* **1981**, *103*, 7694–7696.

(22) (a) Gonzales, J. M.; Cox, R. S., III; Brown, S. T.; Allen, W. D.; Schaefer, H. F., III. *J. Phys. Chem. A* **2001**, *105*, 11327–11346. (b) Gonzales, J. M.; Pak, C.; Cox, R. S.; Allen, W. D.; Schaefer, H. F., III; Csaszar, A. G.; Tarczay, G. *Chem.—Eur. J.* **2003**, *9*, 2173–2192. (c) Gonzales, J. M.; Allen, W. D.; Schaefer, H. F., III. *J. Phys. Chem. A* **2005**, *109*, 10613–10628.

(23) Hoz, S.; Basch, H.; Wolk, J. L.; Hoz, T.; Rozental, E. *J. Am. Chem. Soc.* **1999**, *121*, 7724–7725.

(24) Beak, P.; Bonham, J.; Lee, J. T., Jr. *J. Am. Chem. Soc.* **1968**, *90*, 1569–1582.

(25) (a) Marcus, R. A. *J. Am. Chem. Soc.* **1969**, *91*, 7224–7225. (b) Albery, W. J.; Kreevoy, M. M. *Adv. Phys. Org. Chem.* **1978**, *16*, 87–157. (c) Shaik, S. S.; Schlegel, H. B.; Wolfe, P. *Theoretical Aspects of Physical Organic Chemistry: The S_N2 Mechanism*; Wiley: New York, 1992.

Scheme 5. Gibbs Energy Profile for the Methylation of the Pyridone Anions with Methyl Chloride (MP2/6-311+G(2d,p), all in kJ mol^{-1})
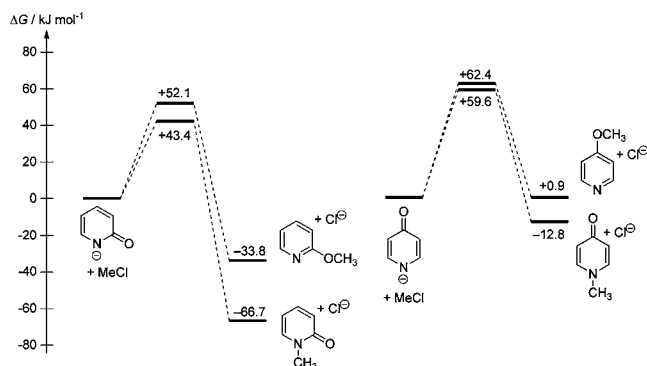
Scheme 6. Selective *N*-Alkylation of 2-Pyridone Anion with Acrylonitrile[26]
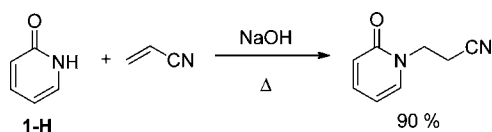
exchange in CH$_3$Cl (38.2 kJ mol^{-1})[15] as formulated in the footnote of Table 8.

The Gibbs energies of activation for the methylation of the pyridone anions **1** and **2** by methyl chloride ($\Delta G^{\ddagger}$) have then been calculated by the Marcus equation (eq 4) from the corresponding intrinsic barriers $\Delta G_0^{\ddagger}$ and the Gibbs energies of reaction ΔG^0 (Table 8).

Discussion

Alkylation of Alkali Salts. Scheme 5 which summarizes the results presented in Table 8, can now be used to rationalize the experimental findings on the reactivities of pyridone anions. In the case of both pyridones, *N*-alkylation is generally preferred thermodynamically, but the preference of the *N*-alkylated pyridone over the isomeric alkoxypyridine is considerably greater in the 2-pyridone than in the 4-pyridone series. The exclusive observation of *N*-attack with highly stabilized carbenium ions ($E < -7$) and Michael acceptors ($-17 < E < -11$) reported in Table 6 and Scheme 4 can be explained by the reversibility of these reactions and the formation of the thermodynamically more stable product. Support for this interpretation comes from the fast dissociation reactions of the adducts which can be calculated from the equilibrium constants in Table 7 and the rate constants of the reactions of the pyridone anions with the quinone methides reported in Tables 2 and 3. Furthermore, the adducts **4-N** and **5-N** obtained from amino substituted benzhydrylium ions were observed to dissociate into the carbenium ions **3** and the pyridone anions **1** and **2** when treated with water.

The exclusive formation of *N*-alkylated products from 2-pyridone anions with acrylonitrile[26] or with related Michael acceptors[16] can analogously be rationalized by the reversibility of these additions (Scheme 6).
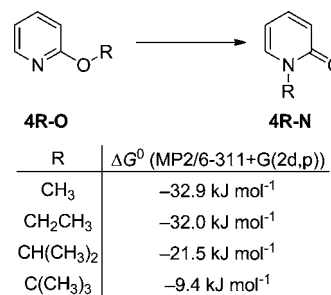
According to Scheme 5, the higher thermodynamic stabilities of the *N*-methylated pyridones ($\Delta\Delta G^0$ term) are also responsible for the lower transition state for *N*-attack, i.e., for the preferred *N*-alkylations of the pyridone anions under conditions of kinetic

Table 9. Effect of Alkylating Agent and Counterion on the *N/ O*-Alkylation Ratio in DMF[4]

entry	electrophile	salt	*N/O*-ratio
1	MeI	**1-Na**	95:5
2	MeI	**1-K**	92:8
3	PhCH$_2$Cl	**1-Na**	94:6
4	PhCH$_2$Br	**1-Na**	97:3
5	PhCH$_2$I	**1-Na**	98:2
6	EtI	**1-Na**	69:31
7	iPrI	**1-Na**	30:61^a

^{a} 2-Pyridone was partially recovered.

Scheme 7. Calculated Thermodynamic Difference ΔG^0 for *O*- and *N*-alkylated 2-Pyridones in the Gas Phase

R	ΔG^0 (MP2/6-311+G(2d,p))
CH$_3$	−32.9 kJ mol^{-1}
CH$_2$CH$_3$	−32.0 kJ mol^{-1}
CH(CH$_3$)$_2$	−21.5 kJ mol^{-1}
C(CH$_3$)$_3$	−9.4 kJ mol^{-1}

Scheme 8. Selective *O*- and *N*-Tritylation of Pyridone Salts in Acetonitrile[27]
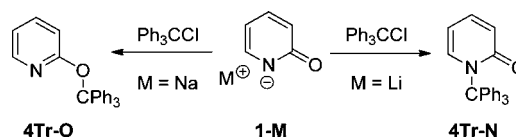
control. As reported by Tieckelmann,[4] the sodium and potassium salt of **1** react with 92−98% nitrogen attack when treated with methyl iodide and different benzyl halides in DMF at room temperature (entries 1−5, Table 9).

MP2/6-311+G(2d,p) calculations show that the thermodynamic preference for *N*-attack shrinks when the steric bulk of the alkylation agent is increased (Scheme 7).

The decreasing *N/O* ratio when turning from MeI to EtI and *i*PrI (entries 1, 6, 7, Table 9) can therefore be explained by the fact that the intrinsically preferred *O*-attack is gaining importance as the $\Delta\Delta G^0$ term, which favors *N*-attack, decreases. Qualitatively speaking: An increase of the size of R introduces more strain into the *N*-alkylated product **4R-N** than in the *O*-alkylated product **4R-O**, and a fraction of this effect is already noted in the corresponding transition states.
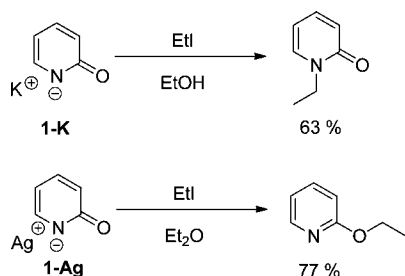
Exclusive *O*-attack was observed, when **1-Na** was treated with the even bulkier tritylating agent Ph$_3$CCl, while **1-Li** gave exclusive *N*-attack under the same conditions (Scheme 8). Since **4Tr-O** was found to isomerize into **4Tr-N** in the presence of Lewis acids, one can conclude that also for tritylations, *N*-attack is thermodynamically favored over *O*-attack. The smaller $\Delta\Delta G^0$ term in favor of *N*-attack (extrapolate data in Scheme 7) cannot any longer overcome the intrinsic preference for *O*-attack.

The exclusive *N*-tritylation of **1-Li** (Scheme 8) cannot be the result of thermodynamic product control because the rearrangement **4Tr-O** to **4Tr-N** is very slow under the reaction conditions. We therefore join Effenberger's rationalization that Li$^+$ blocks the attack at oxygen; obviously this ion-pairing plays a role in

(26) Adams, R.; Jones, V. V. *J. Am. Chem. Soc.* **1947**, *69*, 1803–1805.

(27) Effenberger, F.; Brodt, W.; Zinczuk, J. *Chem. Ber.* **1983**, *116*, 3011–3026.

Scheme 9. Regioselectivities in the Alkylation of Potassium[29b] and Silver[30] Salts of Pyridones

Scheme 10. Comparison of the Thermodynamic Differences of *N*- and *O*-Methylated Ordinary Amides, 2-Pyridones, and 4-Pyridones [Gas Phase, MP2/6-311+G(2d,p)]
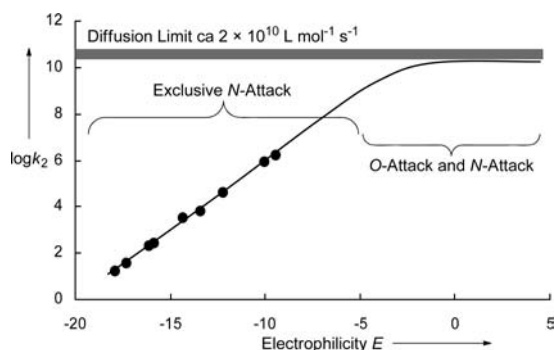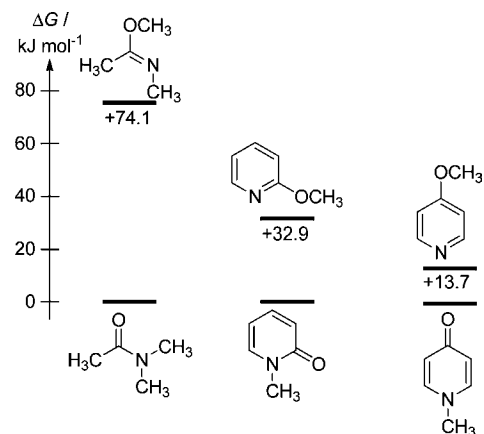

the more concentrated solutions used for the synthesis of **4Tr-N**,[27] though in the highly dilute solutions of **1-K** and **1-Li** in DMSO used for the kinetic investigations, only a slight difference of reactivity was observed (**1** + **3l**, **3i**, Table 2).

Almost exclusive *N*-attack in the reactions of 2- and 4-pyridone anions with 6-(mesyloxymethyl)purines in THF and acetonitrile[28] is also in line with the Marcus model illustrated in Scheme 5. Analogously, Räth obtained *N*-alkylated pyridones in 30−85% yield from the potassium salt of 2-pyridone (**1-K**) and various alkyl halides or dimethyl sulfate (Scheme 9).[29]

Extrapolation of the correlations shown in Figure 2 shows that the reactions of **1** and **2** with carbocations will be diffusion controlled, when their electrophilicty exceeds −2 (Figure 4). As the mechanism of the reactions of the pyridone anions **1** and **2** with the benzhydryl bromides **3a-Br** and **3b-Br** was not clear (S_N1 or S_N2), we have treated **3b-Br** with AgOTf before the pyridone anion was added in order to study the selectivity of the free ditolylcarbenium ion **3b**. The observation of comparable amounts of *O*- and *N*-attack in the reactions of **1** with **3a** (*E* = 5.90) and **3b** (*E* = 3.63) (entries 9, 10, 12 in Table 5) therefore reflects the result of barrierless reactions and cannot be explained by transition state models. Surprisingly, the diffusion-controlled reaction of **2** with **3a** and **3b** occurs exclusively at oxygen, indicating that site-selectivity is not necessarily lost when both competing reactions proceed without barrier.

Alkylation of Silver Salts. Already in 1891, von Pechmann and Baltzer[30] reported that exclusive *N*-attack took place when 2-pyridone was heated with an excess of ethyl iodide, whereas 2-ethoxypyridine (*O*-attack) was isolated when the silver salt of 2-pyridone (**1-Ag**) was employed (Scheme 9). Analogously, Takahasi and Yoneda reported that phenacyl bromide in ethanol react at nitrogen of **1-Na** and at oxygen of **1-Ag**.[31]

Since we have shown that carbocations also give significant amounts of *N*-alkylated pyridones, Kornblum's rationaliza-

tion[3] that the preferred *O*-attack in the presence of silver ions is due to the increased charge of the electrophile cannot hold. As in the case of the ordinary amide anions,[32] silver ions may coordinate to the nitrogen atom of **1** and thus direct the electrophile to the oxygen.[33] The same reason, which is responsible for the formation of isonitriles from alkyl halides and silver cyanide (Ag+ blocks C),[8] thus also controls the site of alkylation of amide and pyridone anions in the presence of silver ions. However, the blocking of nitrogen by silver ions does not occur in the vinylogous amide **2**, as **2-Ag** is attacked at nitrogen by methyl iodide and phenacyl bromide in ethanol.[31]

Conclusion

The large thermodynamic preference of amides over imidates is strongly reduced in the pyridone analogues due to the aromatic character of the *O*-alkylated compounds (Scheme 10). However, *N*-alkylated pyridones are still thermodynamically favored over alkoxypyridines that Michael additions and other reversible reactions generally give *N*-alkylated pyridones.

In kinetically controlled reactions of pyridone anions, *N*-attack is mostly preferred because the thermodynamic contribution to the Gibbs energy of activation, which favors *N*-attack, out-matches the contribution of the intrinsic barriers which favor *O*-attack. Only when $\Delta\Delta G^0$ for *O*- and *N*-attack is becoming small, which is the case for bulky alkylating agents, *O*-attack becomes more favorable.

While diffusion-controlled reactions of the 2-pyridone anion **1** give mixtures of *O*- and *N*-attack, exclusive *O*-attack was observed in diffusion-controlled reactions with the 4-pyridone anion **2**. The *O*-directing effect of silver ions is not due to the

Figure 4. Estimated influence of the diffusion limit on the rate of the reactions of **1** with carbocations and Michael acceptors in DMSO.

(28) Šilhár, P.; Hocek, M.; Pohl, R.; Votruba, I.; Shih, I.-h.; Mabery, E.; Mackman, R. *Bioorg. Med. Chem.* **2008**, *16*, 2329–2366.
(29) (a) Räth, C. *Liebigs Ann. Chem.* **1930**, *484*, 52–64. (b) Räth, C. *Liebigs Ann. Chem.* **1931**, *489*, 107–118.
(30) v. Pechmann, H.; Baltzer, O. *Ber. Dtsch. Chem. Ges.* **1891**, *24*, 3144–3153.
(31) Takahashi, T.; Yoneda, F. *Chem. Pharm. Bull.* **1958**, *6*, 365–369.
(32) Breugst, M.; Tokuyasu, T.; Mayr, H. *J. Org. Chem.* **2010**, *75*, 5250–5258.
(33) (a) Bancroft, D. P.; Cotton, F. A.; Falvello, L. R.; Schwotzer, W. *Inorg. Chem.* **1986**, *25*, 763–770. (b) Bancroft, D. P.; Cotton, F. A. *Inorg. Chem.* **1988**, *27*, 1633–1637. (c) Rawson, J. M.; Winpenny, R. E. P. *Coord. Chem. Rev.* **1995**, *139*, 313–374.

increased positive charge in the electrophile but due to blocking of *N*-attack by coordination with the silver ion.

Experimental Section

Materials. Commercially available DMSO and acetonitrile (both with H$_2$O content <50 ppm) were used without further purification. Water was distilled and passed through a Milli-Q water purification system. The reference electrophiles used in this work were synthesized according to literature procedures.[7] Potassium and tetrabutylammonium salts of **1-H** and **2-H** were prepared by treatment of the corresponding pyridones with KO*t*Bu in ethanol or *n*Bu$_4$NOH in water. The synthetic procedures for **1-K** and **4l-N** are described as representative examples for the product studies. A complete description for the preparation of all other products is given in the Supporting Information.

2-Pyridone-potassium (1-K). 2-Pyridone (1.80 g, 18.9 mmol) was added to a solution of KO*t*Bu (2.00 g, 17.8 mmol) in dry ethanol (25 mL) and stirred for 30 min. The solvent was evaporated at low pressure and the solid residue was washed several times with dry diethyl ether to afford 2-pyridone potassium (**1-K**, 2.20 g, 16.5 mmol, 93%) as a colorless solid. ^{1}H NMR (d_6-DMSO, 400 MHz) δ = 5.81−5.84 (m, 2 H), 6.94−6.98 (m, 1 H), 7.60−7.62 (m, 1 H). ^{13}C NMR (d_6-DMSO, 101 MHz) δ = 103.9 (d), 113.8 (d), 136.0 (d), 147.7 (d), 173.0 (s).

1-((3,5-Di-*tert*-butyl-4-hydroxyphenyl)(*p*-tolyl)methyl)pyridin-2(1*H*)-one (4l-N). 2-pyridone-potassium (**1-K**, 63.8 mg, 0.479 mmol) was dissolved in dry DMSO (5 mL) and a solution of **3l** (147 mg, 0.477 mmol) in DMSO (5 mL) was added. The mixture was stirred for 15 min before 0.5% acetic acid (∼50 mL) was added. The mixture was extracted with dichloromethane (3 × 40 mL) and the combined organic phases were washed with saturated NaCl-solution (3 × 50 mL), dried over Na$_2$SO$_4$ and evaporated under reduced pressure. Purification by column chromatography on silica gel yielded 1-((3,5-di-*tert*-butyl-4-hydroxyphenyl)(*p*-tolyl)methyl)pyridin-2(1*H*)-one (**4l-N**, 170 mg, 0.421 mmol, 88%) as colorless crystals; mp 164−165 °C (from CHCl$_3$/pentane). ^{1}H NMR (CDCl$_3$, 599 MHz) δ = 1.35 (s, 18 H, 12-H), 2.33 (s, 3 H, 10-H), 5.23 (s, OH), 6.10−6.12 (m, 1 H, 14-H), 6.62 (d, ^3J = 9.1 Hz, 1 H, 16-H), 6.90 (s, 2 H, 3-H), 7.01 (d, ^3J = 8.0 Hz, 2 H, 7-H), 7.12−7.16 (m, 3 H, 8-H, 13-H), 7.29−7.32 (m, 1 H, 15-H), 7.38 (s, 1H, 5-H). ^{13}C NMR (CDCl$_3$, 151 MHz) δ = 21.1 (q, C-10), 30.2 (q, C-12), 34.4 (s, C-11), 61.9 (d, C-5), 105.5 (d, C-14), 120.7 (d, C-16), 125.6 (d, C-3), 128.5 (d, C-7), 129.1 (s, C-4), 129.3 (d, C-8), 136.0 (d, C-13), 136.1 (s, C-2), 136.5 (d, C-13), 137.3 (s, C-9), 138.9 (d, C-15, 153.4 (s, C-1), 162.7 (s, C-17); numbering according to page S8 in the Supporting Information. IR (neat, ATR) $\tilde{v}$ = 3377 (w), 2959 (m), 2922 (m), 2870 (m), 1658 (vs), 1574 (m), 1538 (m), 1432 (m), 1230 (m), 1222 (m), 1142 (w) 1065 (m), 1020 (w), 892 (w), 874 (w), 796 (w), 760 (m), 732 (w). HR-MS (ESI) [M − H]$^-$: *m/z* calcd for [C$_{27}$H$_{32}$NO$_2$]$^-$: 402.2439; found: 402.2447.

Kinetics. As the reactions of colored benzhydrylium ions or quinone methides with colorless pyridone anions **1** and **2** result in colorless products, the reactions could be followed by UV−vis spectroscopy. Slow reactions ($\tau_{1/2}$ > 10 s) were determined by using conventional UV/vis-spectrophotometers. Stopped-flow techniques were used for the investigation of rapid reactions ($\tau_{1/2}$ < 10 s). The temperature of all solutions was kept constant at 20.0 ± 0.1 °C during all kinetic studies by using a circulating bath thermostat. In all runs the nucleophile concentration was at least 10 times higher than the concentration of the electrophile, resulting in pseudo-first-order kinetics with an exponential decay of the electrophile's concentration. First-order rate constants k_{obs} were obtained by least-squares fitting of the absorbance data to a single-exponential $A_t = A_0 \exp(-k_{obs}t) + C$. The second-order rate constants k_2 were obtained from the slopes of the linear plots of k_{obs} against the nucleophile's concentration.

Determination of Equilibrium Constants. Equilibrium constants were determined by UV/vis spectroscopy by adding small volumes of stock solutions of the potassium salts of 2- or 4-pyridone (**1-K** and **2-K**) to solutions of the quinone methides in DMSO. The decay of the electrophiles' absorbances was monitored, and when the absorbance was constant (typically after less than a minute), another portion of the nucleophile was added. This procedure was repeated several times. In order to determine the equilibrium constants K, the molar absorptivities ε of the electrophiles were determined from the initial absorbance, assuming the validity of Lambert−Beer's law.

Quantum Chemical Calculations. Free energies G_{298} were calculated at MP2/6-311+G(2d,p) or B3LYP/6-31+G(d,p) level of theory. Thermal corrections to 298.15 K have been calculated using unscaled harmonic vibrational frequencies. All calculations were performed with Gaussian 03.[34]

Supporting Information Available: Details of kinetic experiments and product studies, archive entries for the MP2 calculations, CIF file for **4l-N**, complete ref 34 (reference[6] in SI). This material is available free of charge via the Internet at http://pubs.acs.org.

JA106962U

(34) Frisch, M. J.; et al. *Gaussian 03*, Revision E.01; Gaussian, Inc.: Wallingford, CT, 2004; see reference 6 in the Supporting Information.